Application of AUV to Track a Maneuvering Target

S. Koteswara Rao and Kausar Jahan

Abstract In this research work, a target maneuvering in its course is tracked using Aerial Unmanned Vehicle (AUV) in three-dimensional space making use of bearing angle, range, and elevation angle measurements. An Extended Kalman filtering algorithm is considered for processing noise altered measurements. An algorithm that uses chi-square distribution is proposed for the detection of any maneuver in target parameters. The statistics about the estimated target parameters are provided to armament administration with the help of a communication arrangement like a global positioning system. Details of mathematical modeling for simulating and implementation of the target and observer paths and outcomes are presented in this work.

Keywords Extended Kalman filter · Estimation · Motion analysis of maneuvering target · Three-dimensional tracking · Aerial unmanned vehicle

1 Introduction

Aerial unmanned vehicle (AUV) is a harmless inflight warfare vehicle present in recent times. AUV is an automaton system hovering in the air mostly used for tracking a target. Parameters that are used to track the target, like bearing, range, and elevation are detected by sending radio waves. AUV these days are furnished with global positioning systems so that the armament administration system of AUV keeps track of it. The armament administration system may be an aircraft in the air or a ship on the surface. Data observed from AUV is directed to the armament administration system with the help of a global positioning system so that the armament administration system will get to know the target's location and path and to release armament in that way. The most common Extended Kalman filter (EKF) algorithm is used for tracking the target. Parameters representing target motion at prolonged ranges are mostly nonlinear. Consequently, EKF is thought based on balancing and speedily converging filter difficulties arising in the Kalman filter [1, 2].

S. K. Rao · K. Jahan (✉)
Department of Electronics and Communication Engineering, Koneru Lakshmaiah Education Foundation, Vaddeswaram, Guntur, Andhra Pradesh, India
e-mail: kausar465@ieee.org

V. Bhateja et al. (eds.), *Computer Communication, Networking and IoT*, Lecture Notes in Networks and Systems 197, https://doi.org/10.1007/978-981-16-0980-0_10

Target tracing is conducted utilizing EKF [3–7]. In this research, the major involvement is tracing a target that is maneuvering in course, as advised in [4, 5]. Observing the residual plot of the bearing target alone cannot visualize. So, the target maneuver is detected by the residuals obtained from a random sequence with zero-mean using chi-square distribution in the gliding window. An innovation that is square and normalized is utilized to detect if the target is under maneuver or not. For obtaining the finest result for the period of target maneuver, an ample quantity of plant noise is tallied to the plant noise covariance matrix. Once the maneuver is concluded, plant noise is dropped back.

The relation of target state elements is nonlinear to the observations (bearing and elevation), which makes the process more nonlinear in nature. So, the Kalman filter that is optimal for the linear process is not applicable for 3-D tracking of the target. For minimalism of the complexity in method, the target moving with steady speed and maneuvering only in its course angle is presumed. The system noise measured is white Gaussian noise delivered because of ruckus in the target's velocity.

Section 2 comprises of precise modeling of the filter and process execution. It also provides the process of detecting the target maneuver execution. Section 3 illustrate the implementation process and the outcomes attained. This paper is concluded in Sect. 4.

2 Mathematical Modeling

2.1 System Model

Contemplate the state vector as follows:

$$X_S(\kappa t) = \left[\dot{x}(\kappa t)\ \dot{y}(\kappa t)\ \dot{z}(\kappa t)\ R_x(\kappa t)\ R_y(\kappa t)\ R_z(\kappa t)\right]^T \tag{1}$$

Here $\dot{x}(\kappa t), \dot{y}(\kappa t), \dot{z}(\kappa t)$. denotes the speed components of target, and $R_x(\kappa t)$, $R_y(\kappa t)$, $R_z(\kappa t)$ are its range components in x, y, and z directions correspondingly. The state vector for subsequent time is calculated using the following equation.

$$X_s(\kappa t + 1) = \emptyset X_s(\kappa t) + b(\kappa t + 1) + \Gamma w(\kappa t). \tag{2}$$

$\emptyset$ is given by

$$\emptyset = \begin{bmatrix} 1\,0\,0\,0\,0\,0 \\ 0\,1\,0\,0\,0\,0 \\ 0\,0\,1\,0\,0\,0 \\ t\;0\,0\,1\,0\,0 \\ 0\;t\;0\,0\,1\,0 \\ 0\,0\;t\;0\,0\,1 \end{bmatrix} \tag{3}$$

Here t is the time frame at which observation is acquired. $b(\kappa t + 1)$ is a deterministic control matrix and is provided by

$$b(\kappa t + 1) = \begin{bmatrix} 0 \\ 0 \\ 0 \\ -(x_0(\kappa t + 1) + x_0(\kappa t)) \\ -(y_0(\kappa t + 1) + y_0(\kappa t)) \\ -(z_0(\kappa t + 1) + z_0(\kappa t)) \end{bmatrix}^{\mathrm{T}} \tag{4}$$

Here x_0, y_0, z_0 denotes the observer location in x, y, and z directions. To lessen the mathematical complication, Y-axis is a reference for computing all the bearing angles and Z-axis for elevation angles. Let $w(\kappa t)$ represent Gaussian process noise.

$$w(\kappa t) = \begin{bmatrix} w_x & w_y & w_z \end{bmatrix}^{\mathrm{T}} \tag{5}$$

The variance of $w(\kappa t)$ is given by

$$E\left[\Gamma(\kappa t) w(\kappa t) w^T(\kappa t) \Gamma^{\mathrm{T}}(\kappa t)\right] = Q\delta_{ij}. \tag{6}$$

where

$$\begin{aligned} \delta_{ij} &= \sigma_w^2 \ (i = \kappa t) \\ &= 0 \quad \text{otherwise} \end{aligned} \tag{7}$$

$$Q = \begin{bmatrix} ts^2 & 0 & 0 & ts^3/2 & 0 & 0 \\ 0 & ts^2 & 0 & 0 & ts^3/2 & 0 \\ 0 & 0 & ts^2 & 0 & 0 & ts^3/2 \\ ts^3/2 & 0 & 0 & ts^3/4 & 0 & 0 \\ 0 & ts^2/2 & 0 & 0 & ts^3/4 & 0 \\ 0 & 0 & ts^2/2 & 0 & 0 & ts^3/4 \end{bmatrix} \tag{8}$$

$$\Gamma(\kappa t) = \begin{bmatrix} t & 0 & 0 \\ 0 & t & 0 \\ 0 & 0 & t \\ t^2/2 & 0 & 0 \\ 0 & t^2/2 & 0 \\ 0 & 0 & t^2/2 \end{bmatrix} \tag{9}$$

$Z(\kappa t)$ denotes the matrix of all observations and is represented as:

$$Z(\kappa t) = \left[R_m(\kappa t)\ B_m(\kappa t)\ \theta_m(\kappa t) \right]^{\mathrm{T}}. \tag{10}$$

Here $R_m(\kappa t)$, $B_m(\kappa t)$ and $\theta_m(\kappa t)$ are measured range, bearing, and elevation.

$$R_m(\kappa t) = R(\kappa t) + \xi_R(\kappa t). \tag{11}$$

$$B_m(\kappa t) = B(\kappa t) + \xi_B(\kappa t). \tag{12}$$

$$Z(\kappa t) = \left[R_m(\kappa t)\ B_m(\kappa t)\ \theta_m(\kappa t) \right]^{T}. \tag{13}$$

Here $R(\kappa t)$, $B(\kappa t)$, and $\theta(\kappa t)$ are the simulated values of the range, bearing angle, and elevation angle.

$$R(\kappa t) = \sqrt{R_x^2(\kappa t) + R_y^2(\kappa t) + R_Z^2(\kappa t)}. \tag{14}$$

$$B(\kappa t) = \tan^{-1}\left(R_x(\kappa t)/R_y(\kappa t)\right).. \tag{15}$$

$$\theta(\kappa t) = \tan^{-1}\left(R_{xy}(\kappa t)/R_Z(\kappa t)\right). \tag{16}$$

where

$$R_{xy} = \sqrt{R_x^2 + R_y^2}. \tag{17}$$

The measurement vector is given by

$$Z(\kappa t) = H(\kappa t) X_s(\kappa t) + \xi(\kappa t). \tag{18}$$

$$H(\kappa t) = \begin{bmatrix} 0\ 0\ 0 & \sin(B)\sin(\theta) & \sin(\theta)\cos(B) & \cos(\theta) \\ 0\ 0\ 0 & \frac{\cos(B)}{R_{xy}} & \frac{-\sin(B)}{R_{xy}} & 0 \\ 0\ 0\ 0 & \frac{\sin(B)\cos(\theta)}{R} & \frac{\cos(\theta)\cos(B)}{R} & \frac{-\sin(\theta)}{R} \end{bmatrix}. \tag{19}$$

And

$$\xi(\kappa t) = \left[\xi_R \ \xi_B \ \xi_\theta\right]^{\mathrm{T}}. \tag{20}$$

2.2 EKF Algorithm

All EKF implementation is as follows.

i. The initial state vector's estimate and its covariance matrix estimate be as of $X(0|0)$ and $P(0|0)$.

ii. For the subsequent time, the state vector is $X_s(\kappa t + 1)$:

$$X_s(\kappa t + 1) = \emptyset(\kappa t + 1|\kappa t) X_{\kappa t}(\kappa t) + b(\kappa t + 1) + \omega(\kappa t). \tag{21}$$

iii. The state vector's covariance matrix for the subsequent time is as follows.

$$P(\kappa t + 1|\kappa t) = \emptyset(\kappa t + 1|\kappa t) P(\kappa t) \emptyset^{\mathrm{T}}(\kappa t + 1|\kappa t) + Q(\kappa t + 1). \tag{22}$$

iv. The gain of the EKF is as follows:

$$G(\kappa t + 1) = P(\kappa t + 1|\kappa t)\emptyset^{\mathrm{T}}(\kappa t + 1|\kappa t) \left[H(\kappa t + 1) P(\kappa t + 1|\kappa t) H^{\mathrm{T}}(\kappa t + 1) + R\right]^{-1} \tag{23}$$

v. The state estimation and its error covariance:

$$X_s(\kappa t + 1|(\kappa t + 1) = X_s(\kappa t + 1|\kappa t) + G(\kappa t + 1)\left[Z(\kappa t + 1) - \hat{Z}(\kappa t + 1)\right] \tag{24}$$

$$P(\kappa t + 1|\kappa t + 1) = [1 - G(\kappa t + 1) H(\kappa t + 1) P(\kappa t + 1|\kappa t)] \tag{25}$$

vi. For the next iteration

$$X_s(\kappa t|\kappa t) = X(\kappa t + 1|\kappa t + 1) \tag{26}$$

$$P(\kappa t|\kappa t) = P(\kappa t + 1|\kappa t + 1) \tag{27}$$

2.3 Target Maneuver Detection

At the time of the target's movement at constant speed and course, the plant noise is a smaller amount. But, as the target starts its maneuver, the plant noise is gradually risen [8, 9]. To increase the plant noise the plant covariance matrix is increased by

multiplying it with a fledge factor of 10 till the target executes maneuvering. When the target maneuver is complete i.e., it attains the required course, the plant noise is brought back to its reduced value. The regulated squared innovation, $\gamma_{\varphi}(\kappa t)$, is calculated as follows.

$$\gamma_{\varphi}(\kappa t) = \varphi^{\mathrm{T}}(\kappa t) S^{-1}(\kappa t + 1)\varphi(\kappa t + 1) \tag{28}$$

where $\varphi(\kappa + 1)$ is

$$\varphi(\kappa t + 1) = Z(\kappa t + 1) - h(\kappa t + 1, X(\kappa t + 1/\kappa t)) \tag{29}$$

Let $S(\kappa t)$ is

$$S(\kappa t + 1) = H(\kappa t + 1)P(\kappa t + 1/\kappa t)H^{\mathrm{T}}(\kappa t + 1) + \sigma^2 \tag{30}$$

$$\mathrm{d}(\xi) = \gamma^{\mathrm{T}} S^{-1} \gamma \geq c \tag{31}$$

where S is diag$\{S(\kappa t)\}$ and

$$\gamma = \varphi 1 \varphi(2) \ldots \varphi \kappa t \quad \gamma = [\varphi(1)\varphi(2) \ldots \varphi(\kappa t)]^{\mathrm{T}} \tag{32}$$

Here c is the threshold with constant value and d is the statistical value of the chi-square distribution. This gliding window of size five samples is chosen for this application.

3 Simulation and Results

Assuming that research is steered at satisfactory ecological circumstances, simulation is conducted on a workstation using Matlab. The trajectories that are followed by target and observer are chosen in Table 1, for performance validation of the process. For instance, scenario 1 defines a target at an opening distance of 2 km away from the spectator, moving with an initial course angle and speed of 170° and 300 m/s correspondingly. The preliminary bearing observed is 0°. The observations, bearing angle, and distance are assumed to be tarnished having a standard deviation in the error of 0.33° (1σ) and 0.01 km (1σ) correspondingly. From 300 s onwards, the target starts its maneuver in course to 295° with a rotating frequency of 3° for every second. The target's initial elevation angle is 0° for ease. The observer is presumed to move with a continual pace of 25 m/s and with 90° course.

The endless accessibility of observations for every time sample is presumed. The actual values of the target position and observer position are generated using Matlab software. Hence, the estimated parameters are authenticated based on the actual modeled parameter values built on specific acceptable standards. The acceptance

Table 1 Scenarios of target and observer positions

Parameters	Scenarios	
	1	2
Opening range of target (m)	2000	3000
The opening bearing of a target (°)	0	0
The opening course of the target (°)	135	170
The course of the target after 300 s (°)	235	295
Speed of target (m/s)	300	400
Elevation of the target (°)	0	0
Speed of observer (m/s)	25	20
The course of the observer (°)	90	90
Bearing angle noise (1σ) (°)	0.33	0.33
Range noise (1σ) (m)	10	10
Elevation angle noise (1σ) (°)	0.33	0.33

measure is preferred based on armament control necessity. The solution is acknowledged or believed to be obtained if inaccuracy in the estimated course is less than 3° and inaccuracy in the estimated speed of the target is less than or equal to 1 m/s.

For scenario 2, the approximations and factual tracks of the target along with that of observer trajectory are shown in Fig. 1. For precision of the notions, Figs. 2 and

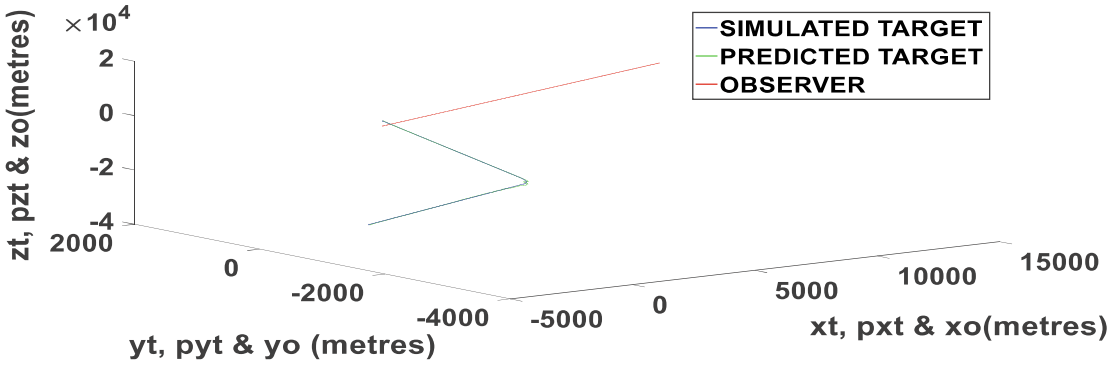

Fig. 1 Simulated and true trajectories of target and observer of scenario 2

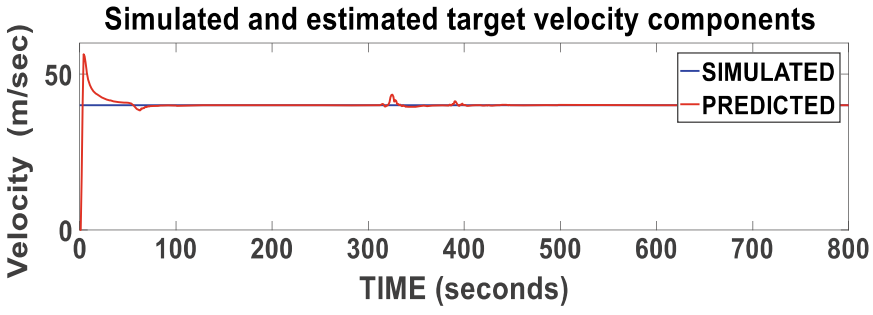

Fig. 2 Factual velocity versus projected velocity of a target for scenario 2

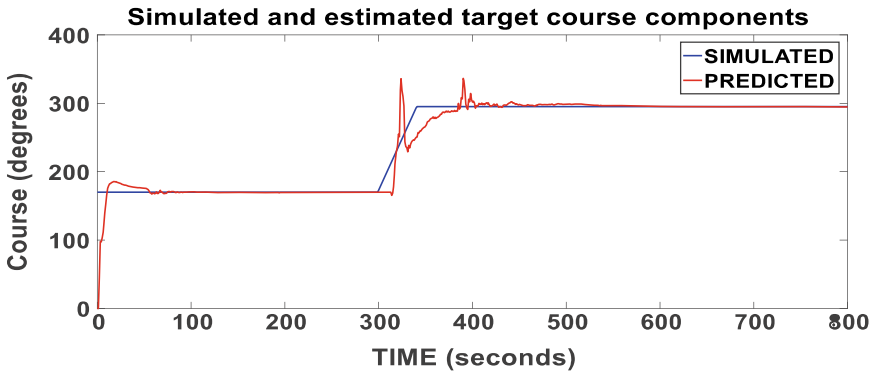

Fig. 3 Factual course versus projected course of a target for scenario 2

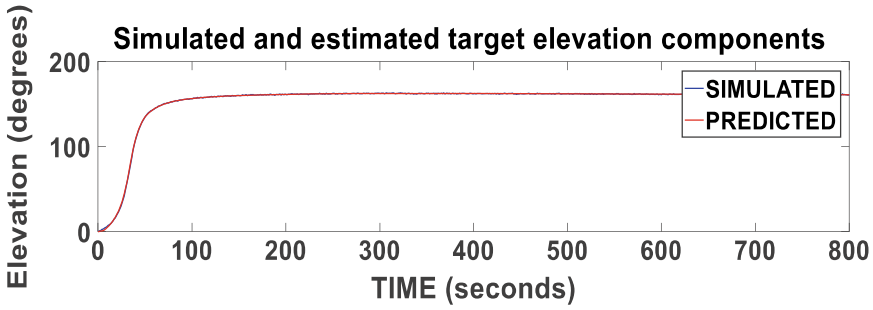

Fig. 4 Factual elevation versus projected elevation of a target for scenario 2

3 shows the actual and estimated course angle and speed of the target for scenario 2 correspondingly. Likewise, the target's actual and estimated elevation angle for the same scenario is depicted in Fig. 4. The result is acknowledged or encountered if the inaccuracies in the estimated course and estimated speed of the target are in the interior of the receiving conditions. Table 2 provides the solution convergence time samples in seconds for the situations provided as in Table 1.

Let us consider scenario 2 to evaluate the algorithm, where the target is maneuvering in its course. The convergence time of outcomes within acceptance criteria

Table 2 Convergence time sample of the solution in seconds

Parameter converged		Scenarios	
		1	2
Earlier to target maneuver	Course	54	67
	Speed	84	43
	Elevation	8	2
	Solution convergence	84	67
Post target maneuver	Course	385	460
	Speed	84	43
	Elevation	8	2
	Solution convergence	385	460

for the estimated course once the target completes the maneuver, is at the 460th-time sample and at the 67th time sample before target maneuvers. As the speed of the target is unchanged, there is only one convergence time, i.e., 43 s, before and after the target maneuver.

4 Conclusion

In this research, an attempt is made to develop an algorithm to track a maneuvering target in a three-dimensional plane. Grounded on the outcomes attained in simulation, EKF is suggested to approximate target parameters in a dynamic model of tracking using AUV systems.

References

1. Edwin Westerfield, E., Dennis Duven, J., Warnke, L.L.: Development of a global positioning system/Sonobuoy system for determining Ballistic missile impact points. John Hopkins APL Techn. Digest **5**, 335—340 (1984)
2. Baker, G.J., Bonin, Y.R.M.: GPS equipped Sonobuoy. https://www.sokkia.com.tw/NOVATEL/Documents/Waypoint/Reports/sonobuoy.pdf. In: Blackman S., Popolli, R. (eds.) Design and analysis of modern tracking systems, Norwood, MA, Artech House (1999)
3. Koteswara Rao, S.: Algorithm for detection of maneuvering targets in bearings only passive target tracking. IEE Proc. Sonar Navig. **146**(3), 141—146 (1999)
4. Koteswara Rao, S.: Modified gain extended Kalman filter with application to bearings only passive maneuvering target tracking. IEE Proc. Radar Sonar Navig. **152**(4), 239—244 (2005)
5. Kavitha Lakshmi, M., Koteswara Rao, S., Subramanyam, K.: Passive Object Tracking Using MGEKF Algorithm. Advances in Intelligent Systems and Computing, vol. 701, pp. 277–287. Springer Nature Singapore Pte Ltd (2018)
6. Jing, D., Han, J., Zhang, J.: A method to track targets in three-dimensional space using an imaging sonar. Sensors (Basel) **18**(7) (2018). https://doi.org/10.3390/s18071992
7. Isbitiren, G., Akan, O.B.: Three-dimensional underwater target tracking with acoustic sensor networks. IEEE Trans. Veh. Technol. **60**(8) (2011)
8. Clark, D.E., Bell, J., de Saint-Pern, Y., Petillot, Y.: PHD filter multi-target tracking in 3D sonar. Europe Oceans 2005, Brest, France, 2005, pp. 265–270. https://doi.org/10.1109/OCEANSE.2005.1511723
9. De Ruiter, H., Benhabib, B.: On-line modeling for real-time 3D target tracking. Mach. Vis. Appl. **21**(17) (2009). https://doi.org/10.1007/s00138-008-0138-y